DETECTION AND EVALUATION OF PATIENT MOTION IN MYOCARDIAL SPECT IMAGING USING MODELING OF PROJECTIONS BY POLYNOMIAL CURVES AND 2D CURVE FITTING

Iraj MOHAMMADI[1], Hossein RAJABI[2], Majid POULADIAN[3], Mahdi SADEGHI[3], Alireza SHIRAZI[4]

Patient motion during myocardial SPECT profusion imaging may result in the formation of artifacts in the reconstructed images. This study attempts to present a method on the basis of modeling image frames through optimum-degree polynomial curves and fitting 2D curves to detect and correct heart motion at pixel and subpixel accuracy. To evaluate our method, NCAT phantom was shifted during data acquisition. Maximum count profile of the heart wall was compared before and after motion correction with that of the motion-free state. This method enables the correction of artifacts formed during motion, preventing the misinterpretation of the results caused by these artifacts.

Keywords: Myocardial SPECT, motion artifact, polynomial curve modeling, motion detection

1. Introduction

Myocardial profusion imaging through Single-photon Emission Computed Tomography (SPECT) is a nuclear medicine procedure used for the diagnosis of coronary artery disease (CAD). Such imaging procedure commonly takes 5-30 minutes to complete, during which time the patient is likely to move [1-2].

Patient movement can be classified into two categories: involuntary and voluntary movements. Involuntary movements include predictable physiological actions of the organs, such as heartbeat, breathing and upward creep of the heart during T1-201 stress test. On the other hand, voluntary movements include non-physiological and non-predictable movements of the body in whole or in part, which the patient exerts for further comfort during the imaging process. Non-voluntary movements commonly result in blurring (increased FWHM) and

[1] Department of Medical Radiation Engineering, Science and Research Branch, Islamic Azad University, Tehran, Iran, e-mail: imohammadi@farabi.tums.ac.ir
[2] Department of Medical Physics, Faculty of Medical Sciences, Tarbiat Modares University, Tehran, Iran
[3] Department of Medical Radiation Engineering, Science and Research Branch, Islamic Azad University, Tehran, Iran
[4] Department of Medical Physics and Biomedical Engineering, Faculty of Medicine, Tehran University of Medical Sciences, Tehran, Iran

reduced image quality. There are different ways to deal with voluntary and involuntary movements. Involuntary movements are always there and follow a relatively constant and predictable periodic pattern. A common solution for the correction of involuntary movements is segmentation of a periodic movement into different temporal phases and collecting data for each individual phase [3-5].

Voluntary (non-physiological) movements, however, occur on a probabilistic basis (10% to 20% of the times) and do not follow any predictable pattern. The general effect of these movements is blurring in the images, which manifests in different conditions as different types of artifact (e.g. decreased counts per pixel, image quality deterioration, border splitting and shape distortion). The resultant artifacts may endanger medical diagnosis [6-8].

Theoretically, a physical movement-detection device could be a challenging solution in the precise detection of movement range and its correction. Such devices may include IR cameras and IR reflectors attached to patient's body [9-10], optical detectors and CCD cameras [11-12]. In a study, the authors measured patient movement through projecting light on patient's face and recording the formed pattern by a camera without attaching any motion detectors on the patient's head [13]. However, due to some potential problems this solution cannot be used in all imaging applications. For instance, in SPECT cardiac imaging using the common protocols, correction is feasible only in the interval between two sequential projections while intra-frame motions cannot be corrected unless the two projections are divided into shorter frames, which is impossible to achieve in existing SPECT imaging systems. Inter-frame motion detection in two sequential frames is possible to achieve through software solutions with lower time and budget constraints.

Various methods have been introduced for the detection and correction of patient movement through the use of data obtained in SPECT studies, including cross-correlation coefficient calculation between the imaged frames and determination of the peak [14]. Nevertheless, the cross-correlation function around the maximum is broad and is affected by noise. This method cannot be used for the detection and correction of gradual movements. The divergent squares method, where the center of the heart is defined as a standard square, is another commonly used procedure. In this method, the center of the heart is traced in sequential images and the image is shifted in reverse on the basis of measured displacements [15]. Attenuation and noise decrease the precision of this method and also it requires the exact specification of the center of rotation (COR). Another method commonly used is optical flow algorithm in which a 2D velocity vector for each pixel in the sequence of images captured by the camera (or in any element of the image matrix) is formed to describe the movement of that element between two sequential frames [16]. The results of the application of this algorithm to SPECT image data obtained from a patient show significant deviation from the actual amount due to vastness of the source. Other methods

used to form motion-free data include multi-head SPECT and 360-degree data acquisition [17] and dual scan [18]. Since some images affected by motion are dropped in these methods, the number of statistical counts decreases and special attention needs to be paid to the error in cross-correlation function for the detection of motion. In addition, the methods have not made their way into common imaging protocols. In another attempt, the researchers determined the center of the mass to correct the pulmonary motion of the heart [19]. In another study, a cross-correlation function was calculated to automatically detect the motions in the captured frames [20]. In addition, linogram/sinogram cross-correlations were used to detect motion in planar and SPECT imaging [21]. In another study, phase-only correlation method was presented to detect motion perpendicular to the detecting system [22]. The major drawback of the latter methods was their dependence on the quality of scan data, including resolution, sampling and noise features that affect motion parameters.

The authors in this study use only the data obtained from the imaging system to present a relatively precise, simple and rapid method to eliminate the effect of noise and other imaging parameters that may affect the timing and motion detection of the heart. First, the summed profile (SP) of the imaged frame matrix is calculated. Then the heart motion is calculated on the basis of an optimal-degree polynomial curve fitted onto vectors corresponding to sequential frames and fitting the 2D curve at the pixel and subpixel accuracy. This method was tested and assessed through applying artificial motions to NCAT chest phantom.

2. Materials and Methods

The present study was conducted using real and simulated images. NCAT phantom was utilized to simulate cardiac imaging of the chest phantom. A 128×128×128 matrix with a 3mm cubic voxel size was used for phantom. Gate's Monte Carlo simulation was used to produce the projection frames. The applied radioactive material was Tc99m. Imaging was performed using the common imaging protocol [23], in which 32 frames were produced in 180° arcs. A 35cm radius of rotation was used. The energy window was set at 140±10% keV and the total count of each projection was 100-150 kilo counts. The used collimator was low energy high-resolution (LEHR). The camera field of view measured 38 cm × 38 cm, magnification was set 1 and planar frames at 64 × 64 pixels were formed, each pixel size being 5.94 mm. To take into account the effects of photon absorption and scatter, these photons were also included in the simulations and scatter correction does not applied. First, the phantoms were imaged without applying any artificial motion. Next, the phantoms were moved according to the defined pattern in 3, 6, 9, 12, 15 and 18 mm amounts (approximately and

respectively 0.5, 1, 2, 2,5 and 3 pixels) in early (at the frame 8th), mid (at frame 16th) and late (at frame 24th) stages of data acquisition.

In addition, the proposed method was applied on real cardiac tomography data, which were randomly selected from the database of two nuclear medicine centers, were used for motion detection and correction.

In order to determine the motion time and measure the motion size, summed profiles were calculated in two perpendicular directions. If we sum all the elements of frame matrix that are in a same row or column, we get a 1D vector that contains all the information on total frame counts corresponding to that row or column count and the information on partial distribution in another category. This is indeed the summed profile. Summed profiles whose elements' values originate from the total count in the image matrix rows for all frames are called the summed linogram (SL) and those originating from the total count in the image matrix columns for all frames are called summed sinograms (SS) (Figure 1). Thus for instance, in 32-frame imaging in a 64 × 64 matrix, SL will have 32 columns and 64 rows and, conversely, SS will have 32 rows and 64 columns. In this way, instead of operating at pixel level, operation is conducted on one row or column array. On the other hand, since we sum together all image matrix elements which are equal in one row or column, a 1D vector will be formed which included relatively large values and the sensitivity to the statistical noise will be reduced. To eliminate noise in determination of motion size, an optimal-degree polynomial curve is used to model the data in each obtained row or column of SP.

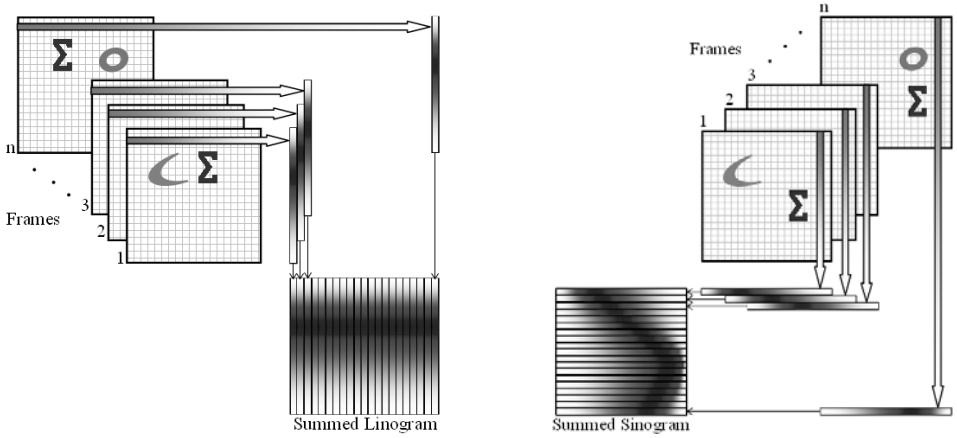

A B

Fig. 1. Calculating SP. A) SL: Each column in the SL corresponds to one projection and the value at every location along a given SL column is equal to the summation of counts in the pixels along the row at the corresponding vertical location. B) SS: Each row in the SS corresponds to one projection and the value at every location along a given SS row is equal to the summation of counts in the pixels along the column at the corresponding horizontal location.

Before calculating the SP, we need to select the region of interest (ROI) in the image frames. Thus, only the counts in the region that include the target organ

(i.e. the heart) will be considered. In visual inspection of the occurrence of motion, deviation from a straight line in SL and occurrence of discontinuity indicate horizontal patient motion along the bed while a deviation from a sine shape in SS and the occurrence of discontinuity suggest patient motion perpendicular to the patient bed.

In order to quantify patient motion, we assume each SL column or each SS row to be a vector. Figure 2A shows the profiles of the data in two adjacent columns in SL which correspond to two sequential image frames. The intensity of noise problem in the images makes the size of the motion difficult to detect. Our proposed method is optimized for the elimination of noise effect and the precise measurement of heart displacement through modeling the imaged frames with an optimum-degree polynomial curve. To do so, first we assume an approximate polynomial curve of least squares for the data in each SL column. We change the polynomial degree from zero to a maximum value (the number of data in each column minus one) and calculate least squares errors for each degree value. Then we select that degree of the polynomial for which the least squares errors are minimized as the optimal degree of polynomial. This process is repeated for each individual frame where each frame is modeled with an optimal-degree polynomial. Since in SPECT imaging the gamma camera registers gamma photons at different angles to produce the image frames and since different tissues occur between the heart and the gamma camera, the effect photon absorption and scattering of the photons is high. In addition, due to statistical nature of radioactive decay and the use of SPECT imaging (through a collimator), the count in each pixel and the noise level in different frames (different SL columns) vary. Therefore, the degree of the modeled polynomial is not necessarily equal to different frames. Figure 2B illustrates that amount of motion can be calculated through modeling the data existing in two adjacent SL columns (corresponding to two sequential frames) with polynomial curve modeling.

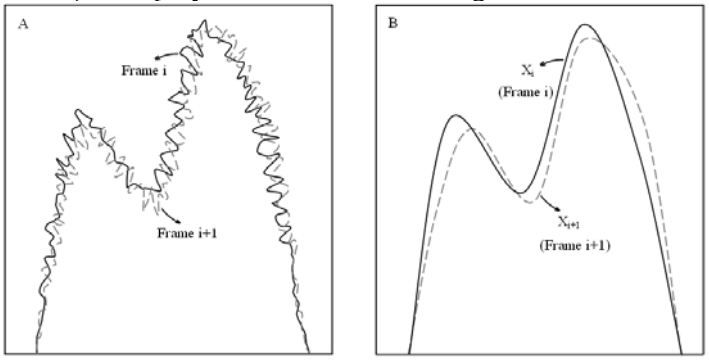

Fig. 2. (A) Profiles drawn from the data in two adjacent columns of the SL corresponding to two sequential image frames. These profiles are heavily smeared by noise, making the correct measurement of motion size difficult. (B) Same profiles modeled by optimum-degree polynomials clearly reveal patient motion. The method used to quantify the motion and determine the precise amount of motion is elaborated in the text.

To estimate the motion size, we calculate the roots of optimum-degree polynomials with two sequential image frames (frames i and i+1) at height k and designate them as R_{kl}^{i} and R_{kl}^{i+1}, respectively (where i is the frame number and l the root number at a given height). Once the roots at higher parts of the curves are calculated, the effects of noise and counts associated with surrounding context and tissues with low radioactivity absorption (e.g. lungs, bones and body) are removed from the calculation of organ (i.e. the heart) motion size.

Even if the patient remains motionless during the imaging process, neither of the corresponding roots in R_{kl}^{i} and R_{kl}^{i+1} will be identical. In other words, the difference between the two corresponding roots is not consistently zero. This is because of the statistical nature of radioactivity decay and the occurrence of different tissues between the heart and the camera at different angles and also due to the variable organ profiles in different image frames. Therefore, if the corresponding root differences at a given height k are positive for some corresponding roots and negative for others, they are excluded from the calculation of the motion size. If this condition holds for all values of k, it means that no motion has occurred between the time intervals of the two frames, suggesting that our proposed method has detected it appropriately.

Now we calculate the mean difference of all corresponding roots through $A_{i,i+1} = \dfrac{\sum_{k=1}^{K}\sum_{l=1}^{n_k}(R_{kl}^{i+1} - R_{kl}^{i})}{\sum_{k=1}^{K} n_k}$, where K is the number of heights at which the curve roots are calculated (the number of horizontal lines in Figure 3) and n_k is the total number of corresponding roots at each height.

The obtained mean provides an early estimate of the motion size between frames i and i+1.To calculate motion size in pixels, we assume that the maximum possible displacement compared to the motionless state of the patient or the organ is d pixels. We then model the column vector associated with frame i in SL with an optimum-degree polynomial curve. However, for frame i+1 first we shift the data in the image matrix of this frame in h pixels ($h = -d, -d+1, ..., 0, ..., d-1, d$) along the rotation axis of the camera (perpendicular to the summation in SL calculation) (in total, 2d+1 times). After each applied shift, we calculate the column vector of this frame in the SL and then obtain the optimum-degree polynomial modeled with the frame i+1 for each value of h (Figure 3 for $h = -d, -d+1, ..., 0, ..., d-1, d$).

Now as stated above, we calculate $A_{i,i+1}$ for each value in $h = -d, -d+1, ..., 0, ..., d-1, d$. Finally, we get 2d+1 number of $A_{i,i+1}$ which we designate as $A_{i,i+1}(h)$. For each value of h where $A_{i,i+1}(h)$ is minimum, motion

size can be determined in pixel: $[a_{i,i+1}, p_{i,i+1}] = \{\min(A_{i,i+1}(h), h\}$, where $p_{i,i+1}$ is a value of h for which $A_{i,i+1}(h)$ has a minimum value (equal to $a_{i,i+1}$). Therefore, $p_{i,i+1}$ is the manifest motion size in pixel, obtained through modeling the myocardial profusion image frame with an optimum-degree polynomial curve.

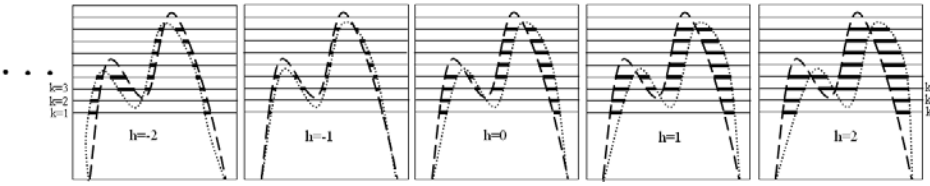

Fig. 3. The solid and dashed lines represent, respectively, optimum-degree polynomial curves modeled on vectors corresponding to the two sequential frames of i and i+1 in a summed profile. The dashed line (which corresponds to the i+1 frame) is obtained after applying a shift of h pixel to the data in the image matrix associated with this frame. For each value of h where the mean root differences of the two curves (the mean sum of bold horizontal lines) has a minimum value, patient motion is calculated in pixel (in this figure, h = -1). To detection motion at subpixel accuracy, we fit a 2D curve with the results of this figure and determine the minimum point of this curve (see text).

Subpixel motion detection is obtained through fitting a 2D curve on the coordinates of the minimum point of the function $A_{i,i+1}(h)$ and the coordinates of two adjacent points. The coordinates of these three points are as follows:

$$\{(A_{i,i+1}(p_{i,i+1}-1), p_{i,i+1}-1); (A_{i,i+1}(p_{i,i+1}), p_{i,i+1}); (A_{i,i+1}(p_{i,i+1}+1), p_{i,i+1}+1)\}$$

The minimum value of this fitted 2D function is an estimate of the motion in subpixel: $s_{i,i+1} = p_{i,i+1} + \dfrac{A_{i,i+1}(p_{i,i+1}+1) - A_{i,i+1}(p_{i,i+1}-1)}{2(2A_{i,i+1}(p_{i,i+1}) - A_{i,i+1}(p_{i,i+1}+1) - A_{i,i+1}(p_{i,i+1}-1))}$

Finally, the detected motion is rounded to the closest value which is a multiple of 0.5 pixel (amount of motion threshold that can cause motion artifact) so that the motion is detected and corrected.

$$r_{i,i+1} = \frac{round(s_{i,i+1} \times 2)}{2}$$

Thus $r_{i,i+1}$ is the manifested motion at subpixel accuracy which is obtained through modeling myocardial profusion image frames with an optimum-degree polynomial curve and fitting a 2D curve onto the results of the modeling.

After data acquisition using our proprietary computer program, the frames were displayed in the cine mode. By drawing guidelines, the program helps the operator to visually inspect the motion. In addition, the summed profiles (SL and SS) are drawn by the program to obtain an estimate of the time and size of the motion on the basis of the location and amount of deviation from the straight line

or a sine curve. Our proprietary program automatically quantifies motion at the pixel and subpixel levels without the need for the operator's intervention.

To evaluate the method, nineteen 32-frame tomography files were obtained from cardiac SPECT simulations using NCAT phantom (one motion-free reference file and 18 motion-applied files at different times (early, mid and late data acquisition stages) with variable amount of motion (from 0.5 pixel to 3 pixels). Cardiac SPECT simulated data were reconstructed using back projection method with Butterworth filter (cut-off=0.35 cycles per pixel, order=5).

Once the images were reconstructed, three slices from the short-axis view of the heart in the apical, medial and basal sections were selected. First, the center of the slice was specified and the maximum count for each slice along its radius with an angular distance of 6 degrees from 0 to 360 degrees was obtained. Next, the mean maximum count was calculated along the radial direction of the three slices. Finally, the maximum count profile was drawn on the basis of angular degrees from zero to 360 degrees (Figure 4). The maximum count profile diagrams for the reference images (motionless) were drawn and compared with those of motion-applied and motion-corrected images. In addition, the maximum count profile of motion-applied images subtracted from maximum count profile of reference images and then the mean value with standard deviation (±SD) was calculated for the subtracted curve. This calculation also done for motion-corrected images. The mean value (±SD) as a measure of the amount of the error occurred, which is dependent on the size and time of motion, is compared with the post-correction mean value (±SD) and displayed in a bar graph.

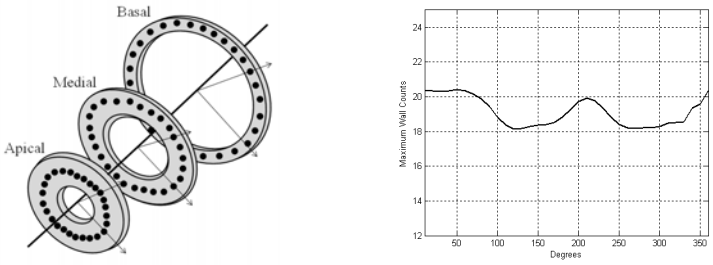

Fig. 4. To evaluate our method in the reconstructed image of the left ventricle, three short-axis view slices were made from the apical, medial and basal parts of the heart. The center of the left ventricle in each slice was specified and the maximum counts in the peripheral region of the left ventricle were measured along the radii of the slices. Next, the mean value of the maximum count in each radius of the three slices was measured in angular degrees.

3. Results

The cardiac SPECT data acquisition was retrieved as planar raw images for visual inspection of motion in cine mode. The results of the application of the program showed that visual inspection of the occurrence of motion is possible

through drawing special guide lines. In addition, the observation of summed profiles (SL and SS) with reference to the location and degree of deviation from the straight line and a sine curve was an indication of the time and size of the motion.

NCAT phantoms were used to evaluate the proposed motion detection and correction method for myocardial SPECT imaging. Maximum count profiles in the peripheral myocardial muscle were compared with each other in the reference (motion-free), motion-affected and motion-corrected states in cardiac SPECT imaging.

Figures 5-7 illustrate the maximum count profiles of the heart wall before applying motion, after 3-18 mm (approximately 0.5 pixel to 3 pixels) motion applied in early (at frame 8th), mid (at frame 16th) and late (at frame 24th) stages of data acquisition and after motion correction. The quantification of the degree to which the data has been corrected is evident. As these figures show, in tomography imaging, where motion had occurred during data acquisition, the maximum counts obtained from a circumferential profile of the heart wall significantly differed from the real values while in the corrected images they were very nearly to the real data before applying motion.

Fig. 8 shows the mean value (±SD) of the subtracted curve of maximum count profile of motion-corrected images and motion-applied images from maximum count profile of reference images. This figure is expected to show the mean maximal counts difference (±SD) for each motion unit (from 0.5 pixel to 3 pixels) for the corrected image as well. However, as shown in Figures 5, 6 or 7, the maximum counts profiles after the motion correction for 0.5 pixel to 3 pixels applied motion are very nearly to each other and to the actual values before applying motion. This implies that the proposed method is capable of detecting and correcting motion independently of the time and size of the motion. Therefore, in Fig. 8, for the sake of simplicity in the report of the results of motion correction (MC), first the mean value of six profiles along each radius is obtained after correcting for 0.5 to 3 pixels of motion to produce a single curve. Next, the mean difference of maximum counts (±SD) was calculated after subtraction of the single curve from the profile of the motion-free image, which can be seen in the MC section of Figure 8.

As Fig. 8 clearly shows, the motion effect in the reconstructed image has been significantly reduced after applying the motion correction program. The success of the developed program and method for the detection and correction of motion in SPECT imaging of the heart from NCAT phantom was attested by a change in the total count in each projection in the imaging protocol and also a change in the dimensions of the ROI and using Hamming, Hann and Butterworth filters for the reconstruction of simulated images. The results are almost similar to those shown in Figures 5-8, which show that motion can be appropriately corrected using the proposed method.

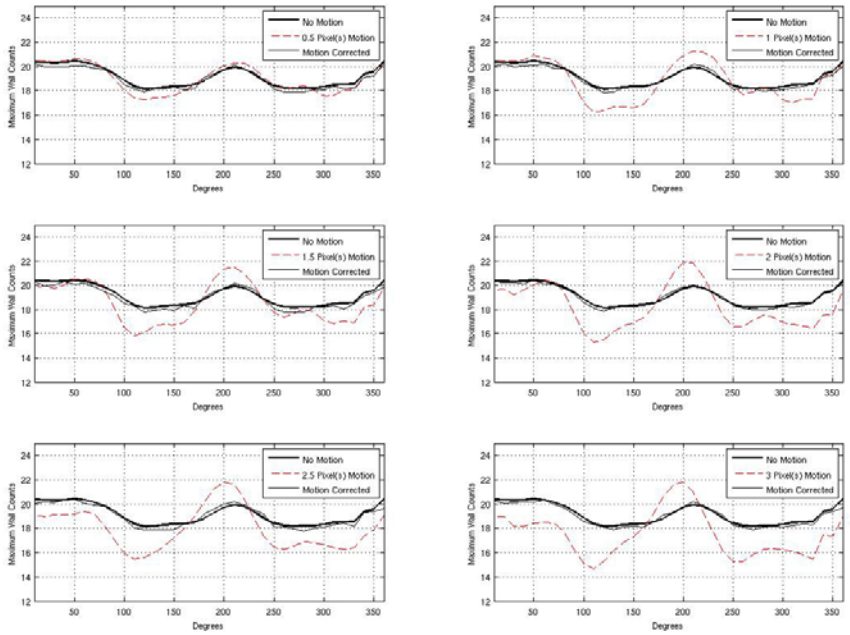

Fig. 5. Maximum count profiles of the heart wall, before applying motion, with 0.5, 1, 1.5, 2, 2.5 and 3 pixels motion in early data acquisition stage (frame 8) and after motion correction.

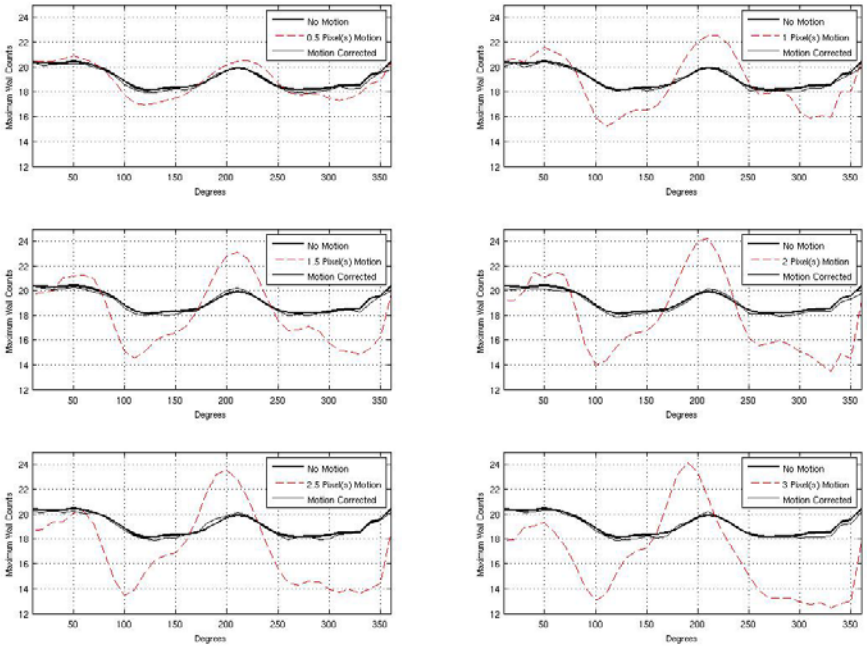

Fig. 6. Maximum count profiles of the heart wall, before applying motion, with 0.5, 1, 1.5, 2, 2.5 and 3 pixels motion in in mid (frame 16) data acquisition stage and after motion correction.

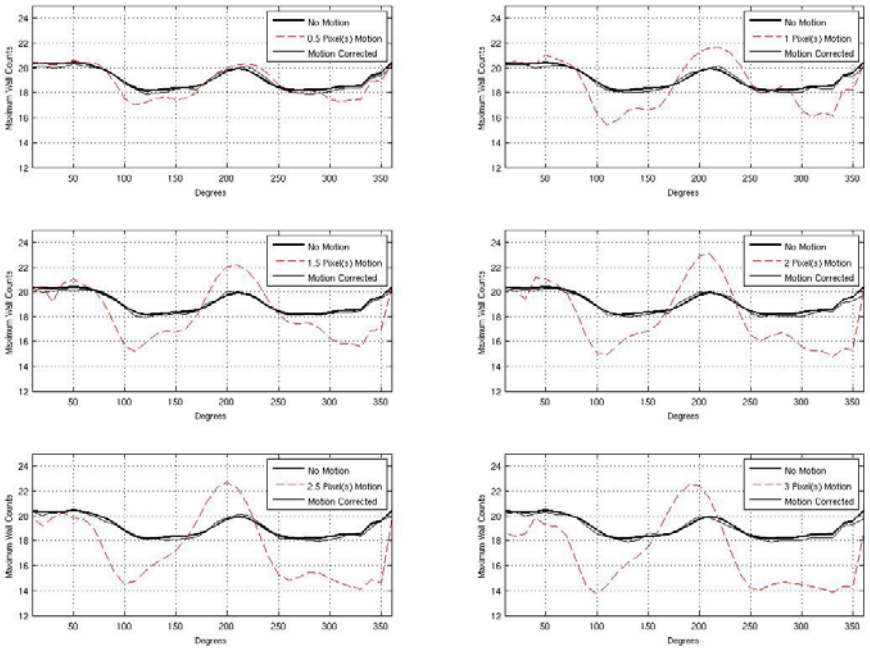

Fig. 7. Maximum count profiles of the heart wall, before applying motion, with 0.5, 1, 1.5, 2, 2.5 and 3 pixels motion in late (frame 24) data acquisition stage and after motion correction.

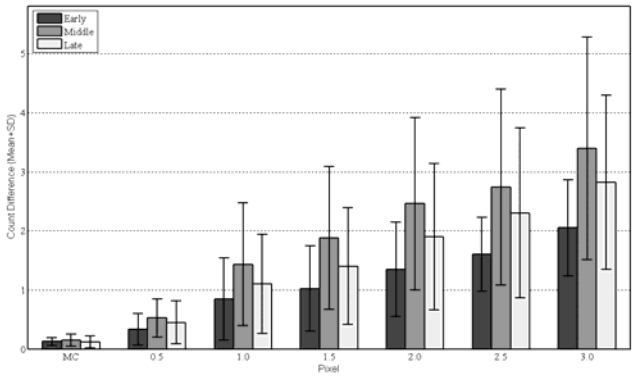

Fig. 8. Mean value (±SD) of the subtracted curve of maximum count profile of motion-corrected images and with 0.5, 1, 1.5, 2, 2.5 and 3 pixels motion in early, mid and late data acquisition stages images from maximum count profile of reference images.

An analysis of the results from the effect of motion in SPECT imaging of myocardial profusion shows that at identical motion times, the error increased as the motion size increased. In addition, we found that the greatest amount of error was due to the motion which occurred in mid data acquisition stage. The error value in late data acquisition stage was larger than that of the early stage of data acquisition process. However, the results of our study show that our method was

successful at detecting and correcting patient motion in SPECT imaging of myocardial profusion independently of the time and size of the motion.

For instance, Figure 9 shows myocardial profusion imaging for a real patient before and after motion correction. The administered radiopharmaceutical agent was Tc-99m-sestaMIBI. A 3 pixels motion occurred in frame 10. Viewed in cine mode, the occurrence of the motion and the examination of the summed profile were verified. Motion size was measured by applying the motion detection program and was subsequently corrected. The success of the method for the measurement of the motion size and correction of the detected motion was confirmed by two nuclear medicine specialists. According to their opinion, images affected by motion artifacts and corrected by this method improved physicians' ability to interpret the images and diagnose likely patient conditions, making an imaging repeat unnecessary.

A)
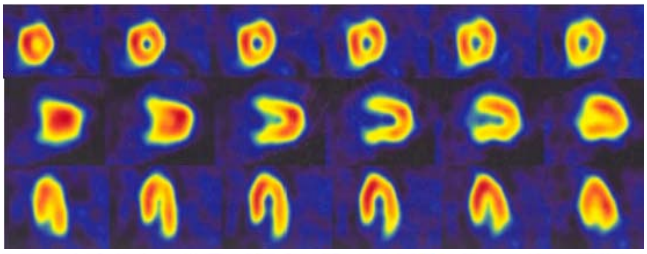
B)
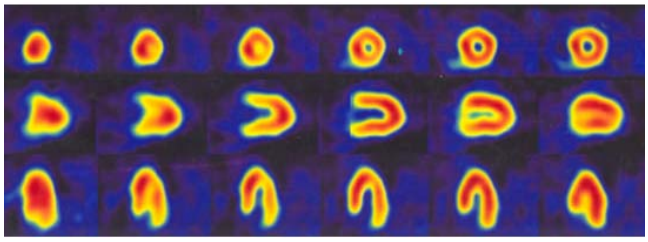

Fig. 9. A number of slices of the myocardial profusion imaging of a patient at rest (A) before motion correction and (B) after motion correction.

4. Discussion

Despite ample briefing to patients to control any movement during medical imaging process and in spite of using fixing instruments, the reconstructed images from nuclear medicine centers are often reported to be of low quality due to patient movement. Therefore, appropriate detection and correction methods can solve this problem significantly and prevent repeating data acquisition and waste of time, and in some cases, patient reinjection.

The visual inspection of projections in cine mode and checking discontinuity in linogram and sinogram to observe possible motion prior to reconstruction are subjective and limited by being operator-dependent [20-21]. The external devices are used to track patient motion during acquisition but using

these devices is not possible to correct intra-frame and organ motions in ordinary myocardial imaging. Moreover, these devices are usually not very simple to operate [9-13]. Most methods based on the data obtained from the imaging system, specially cross correlation methods, are not routinely used protocols in cardiac SPECT imaging or suffer from attenuation and low photon count due to radioactive dose limitations (high noise level) [3, 7, 20-21].

We demonstrated that modeling polynomial curves on existing vectors in the summed profiles that correspond to the obtained image frames can prove useful in detecting the time and size of heart motion in SPECT myocardial profusion imaging. It was shown that patient motion during the imaging process causes incorrect registration of counts in pixel in the reconstructed images. The negative effect of motion in the middle stage of data acquisition is higher than that occurring in the early or late stages. In addition, in angles where the tomography ROI is closer to the gamma camera, motion causes a much more deteriorating effect on image quality. In the real data acquired in myocardial profusion imaging, patient motion is noticeably prevalent. This is especially marked in single-head gamma camera SPECT systems due to a lengthier imaging process. However, it should be noted that in dual-head gamma camera SPECT systems, a single instance of motion affects two frames, resulting in more destructive effects on images compared to single-head systems.

5. Conclusion

In conclusion, through polynomial curve modeling method, cardiac motion was detected and corrected. The method uses only the projection data available from the emission tomography scan. The implementation of this method shows a significant improvement of the quality of the reconstructed cardiac images. Our future research will focus on the evaluation of the present method in various clinical conditions.

REFERENCES

[1]. *Hendel RC, Abbott BG, Bateman TM, Blankstein R, Calnon DA, Leppo JA, et al.* "The role of radionuclide myocardial perfusion imaging for asymptomatic individuals", J Nucl Cardiol **vol. 18**, 2011, pp. 3-15

[2]. *Loong c, Anagnostopoulos c.* "Diagnosis of coronary artery disease by radionuclide myocardial perfusion imaging", Heart, **vol. 90**, 2004, pp. 2-9

[3]. *Niu X, Yang Y, Jin M, Wernick MN, King MA.* "Effects of motion, attenuation, and scatter corrections on gated cardiac SPECT reconstruction", Med Phys, **vol. 38**, 2011, pp. 6571-6584

[4]. *Yu-Wen Yang, Jyh-Cheng Chen, Xin He, Shyh-Jen Wang, Benjamin M. W. Tsui* "Evaluation of respiratory motion effect on defect detection in myocardial perfusion SPECT: a simulation study", IEEE Trans Nucl Sci **vol. 56**, 2009, pp. 671–676

[5]. *Rahmim A, Rousset OG, Zaidi H.* "Strategies for motion tracking and correction in PET", PET Clin, **vol. 2**, 2007, pp. 251–266

[6]. *Wheat JM, Currie GM.* "Incidence and characterization of patient motion in myocardial perfusion SPECT", J Nucl Med Technol, **vol. 32**, 2004, pp. 60-65

[7]. *Massardo T, Jaimovich R, Faure R, Muñoz M, Alay R, Gatica H.* "Motion correction and myocardial perfusion SPECT using manufacturer provided software. Does it affect image interpretation?", Eur J Nucl Med Mol Imaging, **vol. 37**, 2010, pp. 758-764

[8]. *Fitzgerald J, Danias PG.* "Effect of motion on cardiac SPECT imaging: recognition and motion correction", J Nucl Cardiol, **vol. 8**, 2001, pp. 701-706

[9]. *Beach RD, Pretorius PH, Boening G, Bruyant PP, Feng B, Fulton RR, et al.* "Feasibility of stereo-infrared tracking to monitor patient motion during cardiac SPECT imaging", IEEE Trans Nucl Sci, **vol. 51**, 2004, pp. 2693-2698

[10]. *Ahmad Bitarafan, Hossein Rajabi, Bernhard Gruy, Feridoon Rustgou, Ali Akbar Sharafi, Hasan Firoozabady, et al.* "Respiratory motion detection and correction in ECG-gated SPECT: a new approach" Korean J Radiol, **vol.9**, 2008, pp. 490–497

[11]. *McNamara JE, Pretorius PH, Johnson K, Mukherjee JM, Dey J, Gennert MA, et al.* "A flexible multicamera visual tracking system for detecting and correcting motion induced artifacts in cardiac SPECT slices", Med Phys, **vol. 36**, 2009, pp. 1913-1923

[12]. *Mukherjee JM, McNamara JE, Johnson KL, Dey J, King MA.* "Estimation of rigid body and respiratory motion of the heart from marker tracking data for SPECT motion correction", IEEE Trans Nucl Sci, **vol. 56**, 2009, pp. 147-155

[13]. *Olesen OV, Paulsen RR, Højgaard L, Roed B, Larsen R.* "Motion tracking for medical imaging: a nonvisible structured light tracking approach", IEEE Trans Med Imaging, **vol. 31**, 2012, pp. 79-87

[14]. *Eisner RL, Noever T, Nowak D, Carlson W, Dunn D, Oates J, et al.* "Use of cross-correlation function to detect patient motion during SPECT imaging", J Nucl Med, **vol. 28**, 1987, pp. 97-101

[15]. *Geckle WJ, Frank TL, Links JM, Becker LC.* "Correction for patient and organ movement in SPECT: application to exercise thallium-201 cardiac imaging", J Nucl Med, **vol. 29**, 1988, pp. 441-450

[16]. *Noumeir R, Mailloux GE, Lemieux R.* "Detection of motion during tomographic acquisition by an optical flow algorithm", Comput Biomed Res, **vol. 29**, 1996, pp. 1-15

[17]. *Ivanovic M, Weber DA, Loncaric S, Pellot-Barakat C, Shelton DK.* "Patient motion correction for multicamera SPECT using 360 degree acquisition/detector", Proc IEEE Nuclear Science Symp, **vol. 2**, 1997, pp. 989–993

[18]. *Passalaqua AM, Narayanaswamy R.* "Patient motion correction of SPECT images: dual scan approach", Nuclear Science Symposium and Medical Imaging Conference, **vol. 3**, 1994, pp. 1270-1274

[19]. *Bruyant PP, King MA, Pretorius PH.* "Correction of the respiratory motion of the heart by tracking of the center of mass of thresholded projections: a simulation study using the dynamic MCAT phantom", IEEE Trans Nucl Sci, **vol. 49**, 2002, pp. 2159-2166

[20]. *Bai C, Maddahi J, Kindem J, Conwell R, Gurley M, Old R.* "Development and evaluation of a new fully automatic motion detection and correction technique in cardiac SPECT imaging", J Nucl Cardiol, **vol. 16**, 2009, pp.580-589

[21]. *Saeed Sarkar, Mohammad A. Oghabian, Iraj Mohammadi, Alireza Mohammadpour, Arman Rahmim* "A Linogram/Sinogram cross-correlation method for motion correction in planar and SPECT imaging", IEEE Trans Nucl Sci, **vol. 54**, 2007, pp. 71-79

[22]. *Ando R, Ogawa K.* "Correction of patient movement with a phase-only correlation method in a SPECT study", IEEE Nuclear Science Symposium Conference, 2010, pp. 2298-2302

[23]. *Holly TA, Abbott BG, Al-Mallah M, Calnon DA, Cohen MC, DiFilippo FP, et al.* "Single photon-emission computed tomography ASNC imaging guidelines for nuclear cardiology procedures", J Nucl Cardiol, **vol. 17**, 2010, pp. 941-973